Energy & Environmental Science

PAPER

View Article Online
View Journal | View Issue

Cite this: *Energy Environ. Sci.*, 2019, **12**, 2765

Modular engineering for efficient photosynthetic biosynthesis of 1-butanol from CO_2 in cyanobacteria†

Xufeng Liu, Rui Miao, Pia Lindberg and Peter Lindblad *

Received 16th April 2019,
Accepted 16th July 2019

DOI: 10.1039/c9ee01214a

rsc.li/ees

Cyanobacteria are photoautotrophic microorganisms which can be engineered to directly convert CO_2 and water into biofuels and chemicals *via* photosynthesis using sunlight as energy. However, the product titers and rates are the main challenges that need to be overcome for industrial applications. Here we present systematic modular engineering of the cyanobacterium *Synechocystis* PCC 6803, enabling efficient biosynthesis of 1-butanol, an attractive commodity chemical and gasoline substitute. Through introducing and re-casting the 1-butanol biosynthetic pathway at the gene and enzyme levels, optimizing the 5′-regions of expression units for tuning transcription and translation, rewiring the carbon flux and rewriting the photosynthetic central carbon metabolism to enhance the precursor supply, and performing process development, we were able to reach a cumulative 1-butanol titer of 4.8 g L^{-1} with a maximal rate of 302 mg L^{-1} day^{-1} from the engineered *Synechocystis*. This represents the highest 1-butanol production from CO_2 reported so far. Our multi-level modular strategy for high-level production of chemicals and advanced biofuels represents a blue-print for future systematic engineering in photosynthetic microorganisms.

Broader context

In order to reduce the impact of human activities on climate change, we must address our dependence on fossil resources. Biological systems are able to make molecules identical to petroleum-derived compounds used in fuels and in the chemical industry. This has led to increasing attention on the field of metabolic engineering, where microorganisms are genetically engineered to produce compounds of industrial interest. Most such microbial systems employ heterotrophic organisms fed substrates generated from plant biomass. However, photosynthetic microorganisms could be used to perform direct production of fuels and chemicals from photosynthesis, enabling a more efficient conversion of solar energy and carbon dioxide to desirable products, thus leading to more sustainable processes. Engineered strains of photosynthetic cyanobacteria can make many different compounds on a proof-of-concept level, but few products so far show titers approaching those achieved in heterotrophic organisms. We have systematically engineered the unicellular cyanobacterium *Synechocystis* sp. PCC 6803 to produce 1-butanol. The resulting titers are among the highest for any heterologous product from cyanobacteria, and we show that long-term productivity is feasible. The employed strategy can be used for other products when engineering photosynthetic microorganisms for direct production of solar chemicals and biofuels.

Introduction

The increasing energy demand and concerns about CO_2 emissions and global climate change caused by reliance on fossil fuels as our primary energy source give rise to an urgent requirement for renewable energy, such as biofuels.[1,2] Biofuels, produced from renewable resources or biomass feedstocks by microbial cell factories, are already implemented as drop-in fuels.[1,2] In traditional microbial fermentation processes for biofuel production by heterotrophic microorganisms, including *Escherichia coli* and *Saccharomyces cerevisiae*, bio-based sugar feedstocks are required as the carbon source. Additionally, biodiesel can be obtained from crude plant oils. However, for both cases, extensive processes and large agricultural land areas are needed.[1,2] On the other hand, CO_2 can be directly recycled into biofuels using solar energy by engineered photosynthetic microorganisms, such as cyanobacteria.[3–11] These so called solar fuels and chemicals represent potentially cheaper and more sustainable alternatives to traditional biofuels, with the capacity to replace fossil fuels. A prerequisite for pursuing this option is to develop cyanobacteria as efficient green microbial cell factories for directly producing biofuels and biochemicals.

Microbial Chemistry, Department of Chemistry-Ångström, Uppsala University, Box 523, SE-751 20 Uppsala, Sweden. E-mail: Peter.Lindblad@kemi.uu.se

† Electronic supplementary information (ESI) available. See DOI: 10.1039/c9ee01214a

Systematic metabolic engineering holds great promise to develop microorganisms for optimal production of a wide range of biofuels and biochemicals.[12] For heterotrophic model microorganisms, there are by now decades of experience to build upon, where multiple layers of metabolic engineering have been performed in single microorganisms to successfully manipulate the complex cellular metabolism.[12] In cyanobacteria, efforts have been made in proof-of-concept studies towards tailoring the metabolism to produce solar chemicals and fuels. Previous studies demonstrated the potential of cyanobacteria for high-level production of chemicals derived from pyruvate, including ethanol (5.5 g L^{-1}),[5] isoprene (1.26 g L^{-1})[8] and 2,3-butanediol (2.38 g L^{-1}).[13] However, for higher alcohols (*e.g.* 1-butanol), alkanes, fatty acid esters and other acetyl-CoA-derived products, which act as attractive drop-in biofuels for the transportation sector, the reported titers are significantly lower. Thus, systematic engineering of cyanobacteria metabolism is required to enable efficient production of solar fuels and chemicals.

An effective strategy to launch systematic engineering is to use modular pathway engineering, which allows for efficiently evaluating portions of the overall biosynthetic pathway, then combining these to collectively form an altered and interconnected metabolic network.[14–19] In the present study, we implement for the first time a modular engineering strategy in a photosynthetic organism, using the unicellular cyanobacterium *Synechocystis* PCC 6803 (*Synechocystis*) as the host. The target is complete biosynthesis of 1-butanol from CO_2. This is achieved through four work modules (Fig. 1 and Fig. S1, ESI†): Module 1, introducing and re-casting the 1-butanol biosynthesis by systematic screening of genes and pathways; Module 2, optimizing the 5′-regions of expression units to tune the protein expression levels; Module 3, rewiring the carbon flux by editing the acetate metabolism; and Module 4, rewriting the photosynthetic central carbon metabolism by installing a phosphoketolase (PK) pathway. Modules 1 to 4 were established, optimized and assembled consecutively to improve the 1-butanol production stepwise.

Results and discussion

Introducing and re-casting the 1-butanol biosynthetic pathway (Module 1)

In bacterial metabolism, 1-butanol can be produced *via* four distinct biosynthetic pathways (ESI,† Table S1). In the present study, we firstly introduced and optimized two bacterial 1-butanol biosynthetic pathways, consisting of a redesigned *Clostridium*-derived clostridial pathway[6,20,21] and an artificial reversed β-oxidation pathway which was previously demonstrated in *E. coli*.[22] In both pathways, the biosynthesis of 1-butanol is accomplished by six reactions of reduction and dehydration, using acetyl-CoA as the building blocks and involving multiple acyl-CoA thioester intermediates (Fig. 2a). First, two acetyl-CoA or one acetyl-CoA and one malonyl-CoA initiate the pathways, forming acetoacetyl-CoA catalyzed by acetoacetyl-CoA synthase. In the second step of the pathways, acetoacetyl-CoA is reduced to the corresponding 3-hydroxybutyryl-CoA by 3-hydroxyacyl-CoA dehydrogenase. Then, enoyl-CoA hydratase catalyzes the dehydration of 3-hydroxybutyryl-CoA to crotonyl-CoA in the third step. In the fourth step, crotonyl-CoA hydrogenation is catalyzed by enoyl-CoA reductase to synthesize butyryl-CoA. The reduction from butyryl-CoA to butyraldehyde is then catalyzed by CoA-acylating aldehyde dehydrogenase in the fifth step. Alcohol dehydrogenase (ADH) works as the final step by reducing butyraldehyde into 1-butanol. The two CoA-dependent pathways are basically identical, but they differ in the sequential reduction of acetoacetyl-CoA to form intermediate crotonyl-CoA. While two individual enzymes, PhaB and PhaJ, are required for this conversion in the clostridial pathway, one unique enzyme, FadB, in the reversed β-oxidation pathway can produce crotonyl-CoA *via* enantioselective catalysis. Since both pathways consist of multiple enzymes, the corresponding genes were divided and cloned into three artificial operons, with the genes encoding the last two steps in one operon, the third and fourth steps of the clostridial pathway or the second to the fourth steps of the reversed β-oxidation pathway in another, and the first two steps of the clostridial pathway or the first step of the reversed β-oxidation pathway in a third operon (ESI,† Fig. S2). For each step, genes from different sources were selected and overexpressed with various combinations to systematically compare their efficiency for 1-butanol production.

In *Synechocystis*, the intermediates acetoacetyl-CoA and (*R*)-3-hydroxybutyryl-CoA are endogenously generated for poly-3-hydroxybutyrate (PHB) accumulation[23] (Fig. 1). Hence, we started by optimizing the downstream exogenous part of both biosynthetic pathways, *i.e.* the conversion of (*R*)-3-hydroxybutyryl-CoA or acetoacetyl-CoA to 1-butanol in the clostridial and the reversed β-oxidation pathways, respectively (Fig. 2a), resulting in 1-butanol producing strains BOH1–15 (ESI,† Fig. S2a and b). For the butyraldehyde forming step, two CoA-acylating aldehyde dehydrogenase-coding genes, *S. enterica pduP*[24,25] and *E. coli mhpF*,[22] were selected. When overexpressed in combination with genes *yqhD*, *ter* and *phaJ* for the clostridial pathway, the *pduP*-expressing strain BOH1 (39.5 mg L^{-1}) generated an almost 5.5 times higher 1-butanol titer than that of the *mhpF*-expressing strain BOH13 (6 mg L^{-1}) (Fig. 2b). This effect might be attributed to the fact that PduP is an oxygen-tolerant enzyme[6] and therefore exhibits better performance in the presence of oxygen evolved through photosynthesis (Fig. 1).

Subsequently, we moved to optimize the last step, catalyzed by ADH (Fig. 2a). To enhance the photosynthetic 1-butanol production in *Synechocystis*, the co-factor preference of the selected catalytic enzymes must be taken into account due to the prevalence of reducing force NADPH,[26] directly generated from the light reactions of photosynthesis (Fig. 1). Therefore, among strains BOH1–8, four NADPH-specific ADHs, including YqhD and YjgB from *E. coli*, and the endogenous Slr1192 and Slr0942,[27] were investigated in the context of both 1-butanol biosynthetic pathways (Fig. 2c). Overexpression of the *Synechocystis* ADH Slr1192, which here has been used for the first time for 1-butanol biosynthesis, resulted in the highest 1-butanol production in both pathways (48.6 mg L^{-1} in strain BOH3 and 10.8 mg L^{-1} in strain BOH7), even though the *E. coli* ADH YqhD has been widely used in engineering microbial cell

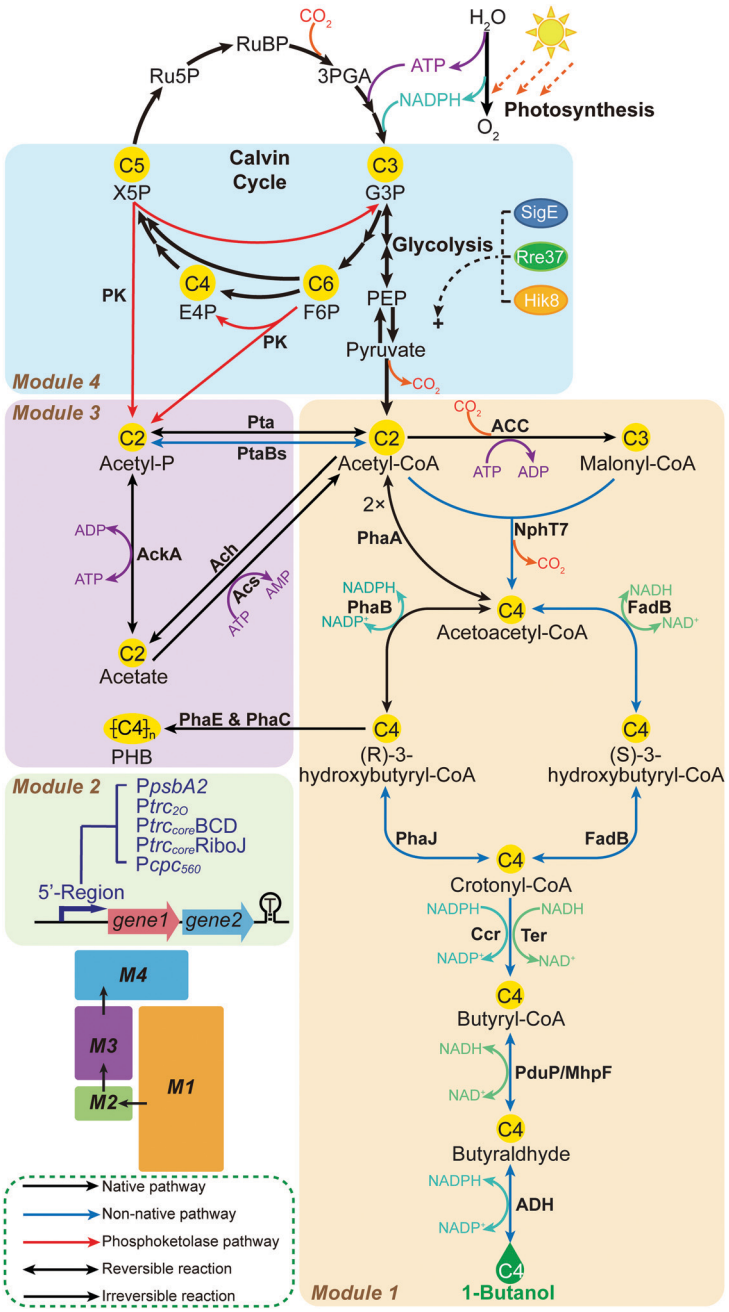

Fig. 1 Biosynthetic scheme for complete biosynthesis of 1-butanol from CO_2 in *Synechocystis* PCC 6803, and the main engineering targets implemented in this study. To establish the boundaries, the engineered biosynthesis is visualized in four Modules, Module 1, 2, 3 and 4, respectively. Metabolite abbreviations: Ru5P, ribulose-5-phosphate; RuBP, ribulose-1,5-bisphosphate; 3PGA, 3-phosphoglycerate; G3P, glyceraldehyde-3-phosphate; F6P, fructose-6-phosphate; E4P, erythrose-4-phosphate; X5P, xylulose-5-phosphate; PEP, phosphoenolpyruvate; acetyl-P, acetyl-phosphate; PHB, poly-3-hydroxybutyrate.

factories for production of higher alcohols,[3,4,6,21,22,28] such as 1-butanol and isobutanol.

Similarly, we attempted to replace the NADH-dependent Ter[20] with NADPH-dependent Ccr[29] to catalyze the conversion of crotonyl-CoA to butyryl-CoA (Fig. 2a). However, no recombinant plasmid harboring the synthetic *ccr-phaJ* operon could be successfully constructed in the intermediate host *E. coli*, and no further comparison was made for the clostridial pathway (ESI,† Fig. S2a). Additionally, with genes *slr1192*, *pduP* and *fadB* overexpressed in the reversed β-oxidation pathway, the 1-butanol titer of the *ccr*-expressing strain BOH11 was similar to that of the *ter*-expressing strain BOH7 (ESI,† Fig. S3). Consequently, the choice between *ccr* and *ter* was not decided, but brought into the next module.

After evaluating the gene candidates for the downstream exogenous part of the two 1-butanol biosynthetic pathways, we turned our attention to optimizing the upstream part starting from central metabolite acetyl-CoA, based on strains BOH3 and BOH7,

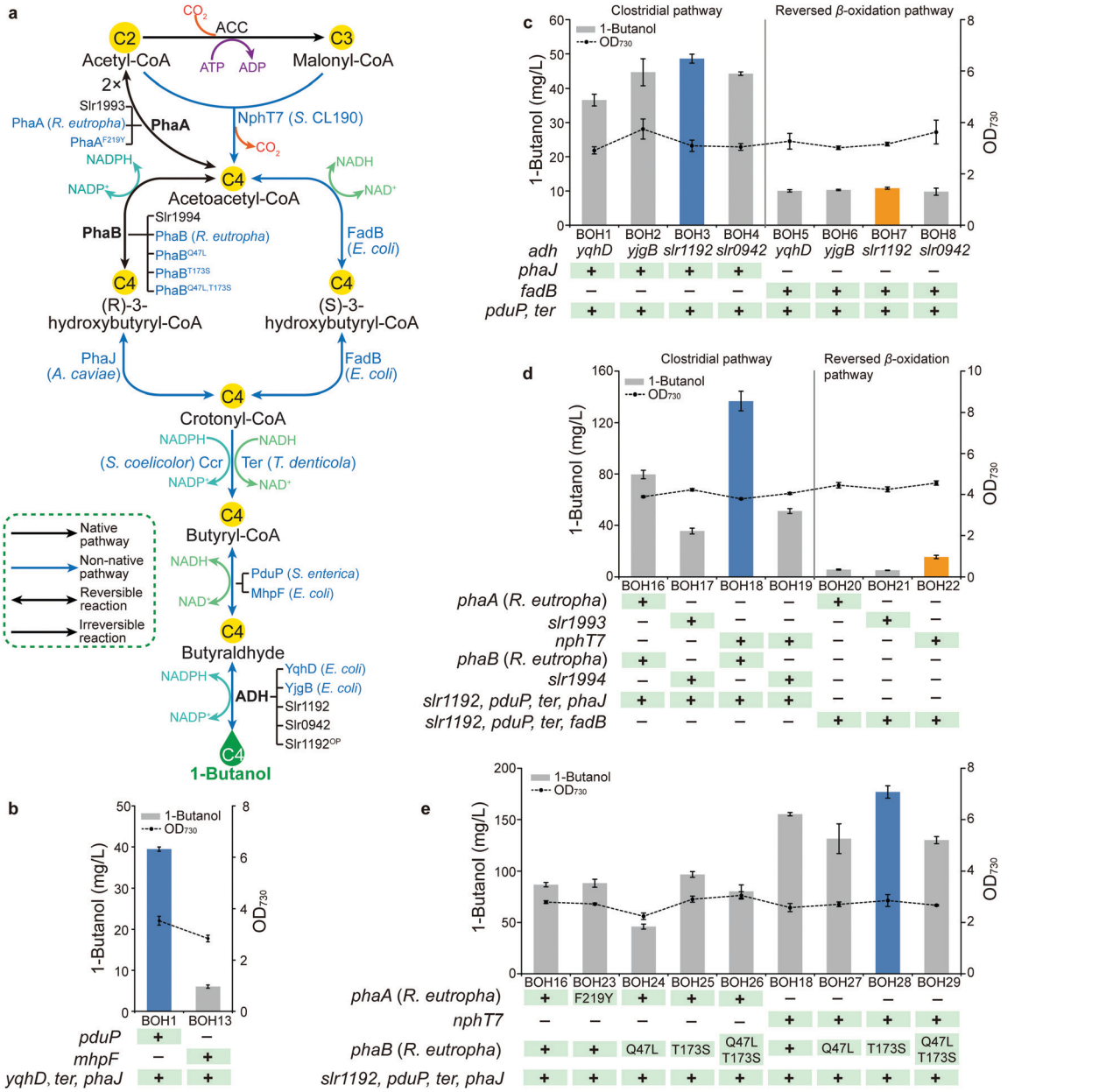

Fig. 2 Introducing and re-casting the 1-butanol biosynthesis in *Synechocystis* PCC 6803 by systematic screening of genes and pathways (Module 1). (a) Biosynthetic scheme of 1-butanol biosynthetic pathways, and the detailed engineering targets implemented in Module 1. Heterologous and endogenous enzymes are shown in blue and black fonts, respectively. (b) 1-Butanol production and cell density of strains BOH1 and BOH13 to compare PduP and MhpF *via* the last four steps of the clostridial pathway. (c) 1-Butanol production and cell density of strains BOH1–8 to compare four ADHs *via* the last four steps of the clostridial pathway and last five steps of the reversed β-oxidation pathway. (d) 1-Butanol production and cell density of strains BOH16–22 to compare the clostridial pathway and the reversed β-oxidation pathway. (e) 1-Butanol production and cell density of strains BOH16, BOH18 and BOH23–29 to compare enzymes modified by amino acid substitutions *via* the clostridial pathway. For (b–e), the time point of the 1-butanol production and cell density is when the maximal in-flask 1-butanol titer is reached. The blue columns indicate the highest 1-butanol production in the clostridial pathway, while the orange columns represent the highest 1-butanol production in the reversed β-oxidation pathway. " +" and "–" indicate with and without target gene engineering, respectively. All data are presented as mean ± SD of biological triplicates.

respectively (Fig. 2a and Fig. S2d–f, ESI†). We found that the clostridial pathway constructed in strains BOH16–19 resulted in significantly higher 1-butanol titers compared with those of the reversed β-oxidation pathway constructed in strains BOH20–22 (Fig. 2d). One reason for the lower production of the reversed β-oxidation pathway may be the co-factor preference in cyanobacteria, which is unfavorable for the NADH-utilizing FadB,[22] while NADPH-dependent PhaB[21] in the clostridial pathway would be preferred (Fig. 2a). Furthermore, PhaB and PhaJ specifically use the (*R*)-stereoisomer of 3-hydroxybutyryl-CoA as an intermediate,[21] instead of the (*S*)-isomer used by FadB,[22] making it impossible for the reversed β-oxidation pathway to

tap into the native carbon flux generated from the endogenous PhaB (Slr1994) (Fig. 2a).

The construction of the initial two steps for the clostridial pathway was inspired by PhaA and PhaB from the PHB production pathway in *Synechocystis*[23] and *Ralstonia eutropha*[30–32] (Fig. 2a), with two different, homologous pairs of *phaA* and *phaB* co-overexpressed. Interestingly, strain BOH16 expressing PhaA and PhaB from *R. eutropha* produced 79.6 mg L^{-1} 1-butanol, which was 1.2× higher than that of strain BOH17 (35.5 mg L^{-1}) overexpressing the endogenous counterparts Slr1993 and Slr1994 (Fig. 2d). For the generation of key intermediate acetoacetyl-CoA, two distinct acetyl-CoA-derived biosynthetic routes were investigated, *i.e.* the PhaA-mediated reversible condensation of two molecules of acetyl-CoA[31] and the irreversible condensation of acetyl-CoA with malonyl-CoA molecules, catalyzed by NphT7[33] (Fig. 2a). Since NphT7 exhibits no thiolysis activity against acetoacetyl-CoA, and one of its substrates, malonyl-CoA, is generated by the irreversible ATP-activated acetyl-CoA carboxylase (ACC), implementation of this activity should establish a driving force to efficiently channel metabolic flux into 1-butanol biosynthesis.[21] As expected, the introduction of NphT7 (strain BOH18) enhanced the formation of 1-butanol to 136 mg L^{-1}, representing a 70% increase compared with that of the PhaA-expressing strain BOH16 (Fig. 2d).

To further increase the 1-butanol production, *R. eutropha* PhaB variants $PhaB^{Q47L}$ and $PhaB^{T173S}$, which have been shown to exhibit improved affinity for cofactor NADPH or substrate acetoacetyl-CoA, respectively,[34] were evaluated *via* the NphT7 route in strains BOH27 and BOH28. An 14% increase in the 1-butanol titer (177 mg L^{-1}) was generated by the $PhaB^{T173S}$-harboring strain BOH28, while introduction of $PhaB^{Q47L}$ (strain BOH27) exerted a negative effect on 1-butanol formation compared with that of strain BOH18 (Fig. 2e). A double mutant $PhaB^{Q47L,T173S}$ was also constructed and overexpressed in strain BOH29. However, the 1-butanol production of strain BOH29 was comparable with that of strain BOH27 expressing $PhaB^{Q47L}$ (Fig. 2e). Furthermore, we tested the 1-butanol biosynthesis *via* the PhaA route in which a $PhaA^{F219Y}$ variant, possessing more than two-fold improved activity *in vitro*,[35] and the PhaB variants were incorporated (strains BOH23–26). As observed for the NphT7 route, only overexpression of $PhaB^{T173S}$ (strain BOH25) enabled a 11% increase of the 1-butanol titer (96.7 mg L^{-1}) compared with that of strain BOH16 (Fig. 2e). Similar protein levels were observed for the PhaA or PhaB homologs (ESI,† Fig. S4).

In Module 1, we implemented, to our knowledge, the first example of a reversed β-oxidation pathway constructed in cyanobacteria. However, the clostridial pathway performed better and resulted in a 1-butanol production of 177 mg L^{-1} (strain BOH28). As the final experiment in Module 1, the *slr1192* gene codon optimized for *Synechocystis* ($slr1192^{OP}$) was generated in order to avoid recombination of overexpressed *slr1192* to its native chromosome site, and its effect on the translation level was examined (ESI,† Fig. S2c). When overexpressed with genes *pduP*, *ter* and *phaJ*, the gene $slr1192^{OP}$ in strain BOH31 led to elevated protein expression and a 25% increase of 1-butanol production to 61.4 mg L^{-1} compared with that of strain BOH3 (ESI,† Fig. S5).

Altogether, a re-cast 1-butanol synthesis pathway using better performing enzymes was obtained in Module 1, with the selection between Ter and Ccr still undetermined (ESI,† Fig. S6). However, the NphT7 route may be limited by the efficiency of the native ACC reaction and malonyl-CoA level. Since PhaA directly uses acetyl-CoA as the source of two-carbon units, PhaA from *R. eutropha* is still a promising alternative enzyme for further engineering.

Optimizing the 5′-regions of expression units (Module 1 + 2)

In Module 1, the 1-butanol biosynthetic genes were organized as three expression units all driven by the same native promoter P*psbA2*[36] (ESI,† Fig. S2), which may cause a limitation for the protein expression and 1-butanol production. Therefore, in Module 2, all the enzyme components of the optimized 1-butanol biosynthetic pathway were subject to systematical tuning at both transcriptional and translational levels. In the former category, two strong constitutive promoters, $Ptrc_{2O}$[37] and $Pcpc_{560}$,[38] were used to regulate the transcript level of genes, while two genetic insulators, BCD (bicistronic design)[39] or RiboJ (self-cleaving ribozyme),[40] were introduced to potentially enhance the protein translation in the latter category (Fig. 3). The genetic insulators were coupled with promoter $Ptrc_{core}$, forming two artificial 5′-regions $Ptrc_{core}$BCD and $Ptrc_{core}$RiboJ, respectively. The performance of the 5′-regions, including promoters, was compared with the original P*psbA2* promoter in each expression unit. Stepwise screening of the three expression units *via* the substitution of promoters or 5′-regions resulted in strains BOH31–57 (Fig. 3). Firstly, while keeping the *ter-phaJ* operon under the control of the P*psbA2* promoter in strains BOH31 to BOH35, we found that a medium expression level of PduP and $Slr1192^{OP}$, under the control of $Ptrc_{2O}$, resulted in the highest 1-butanol titer of 66.3 mg L^{-1} in strain BOH32, representing a 19% increase compared with that of strain BOH31 harboring the P*psbA2-pduP-*$slr1192^{OP}$ unit (Fig. 3a and Fig. S7a, ESI†).

Inspired by this, we moved on to the *ter/ccr-phaJ* operon. In previous studies of the driving forces of the biosynthesis of 1-butanol and other higher alcohols, the implementation of the irreversible activity of NADH-specific Ter is a widely used strategy.[6,16,18,20,21,41] Since this step was recognized as a bottleneck of the pathway,[20] we speculated that the 1-butanol biosynthesis could be improved by the likewise irreversible reaction catalyzed by NADPH-binding Ccr[29] (Fig. 2a), which should be favored by the abundant NADPH content in *Synechocystis*, as noted above. In Module 1, our attempt to express *ccr* and *phaJ* under the P*psbA2* promoter had failed, but by changing the promoters or 5′-regions, four *ccr-phaJ* operons could be successfully constructed (Fig. 3b). Together with five *ter-phaJ* operons, the 1-butanol production performance of these operons was compared based on the previous selection of the $Ptrc_{2O}$-*pduP-*$slr1192^{OP}$ unit (strains BOH40 to BOH47). Among the tested strains, strain BOH45 harboring the $Ptrc_{core}$BCD-*ccr-phaJ* unit had the maximal 1-butanol titer (90.2 mg L^{-1}) (Fig. 3b). Consistent with the titer, the expression levels of Ccr and PhaJ were the highest in this strain (ESI,† Fig. S7b). In the previous screening, only a medium expression level of PduP and $Slr1192^{OP}$ was achieved from the $Ptrc_{2O}$-*pduP-*$slr1192^{OP}$

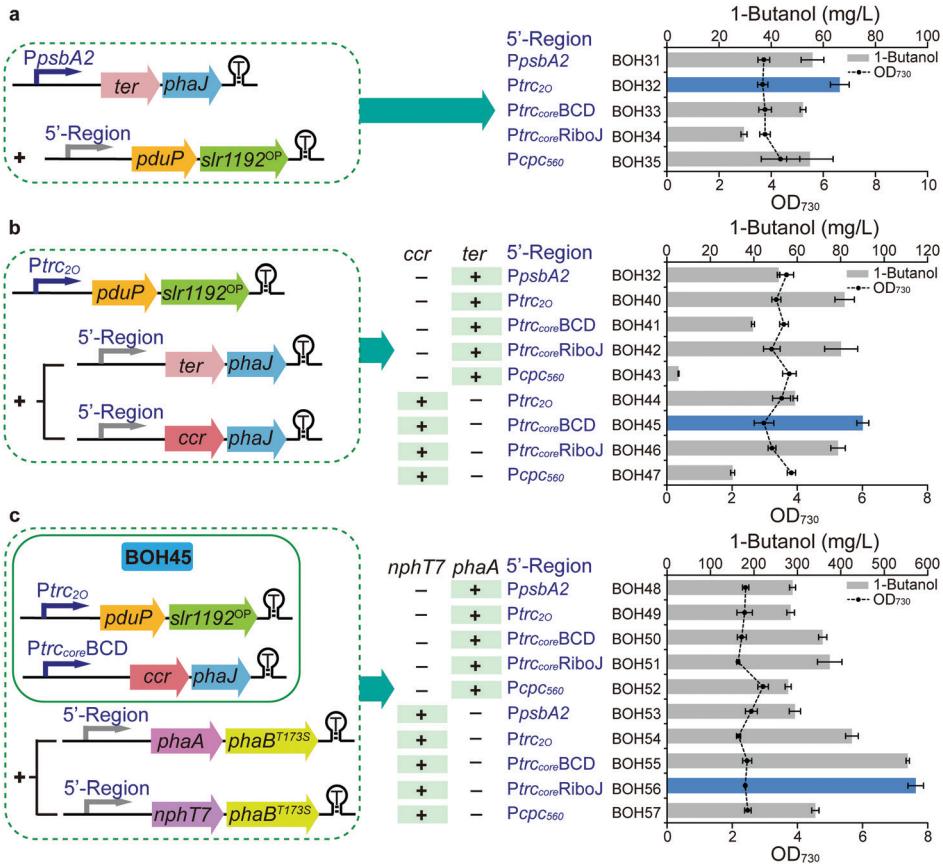

Fig. 3 Systematic evaluation and optimization of the 5′-regions of expression units (Module 1 + 2) in *Synechocystis* PCC 6803. (a) 1-Butanol production and cell density of strains BOH31–BOH35 to screen the 5′-regions of the *pduP-slr1192*^{OP} operon *via* the last four steps of the clostridial pathway. (b) 1-Butanol production and cell density of strains BOH32 and BOH40–47 to screen the 5′-regions of the *ter-phaJ* and *ccr-phaJ* operons *via* the last four steps of the clostridial pathway. (c) 1-Butanol production and cell density of strains BOH48–57 to screen the 5′-regions of the *nphT7-phaB*^{T173S} and *phaA-phaB*^{T173S} operons *via* the clostridial pathway. For (a–c), the time point, colored columns, "+", "−" and other detailed annotations are as described in the Fig. 2(b–e) legend. All data are presented as mean ± SD of biological triplicates. Illustration of the expression units in the strategy designed for 5′-region screening is show on the left of each panel.

unit. However, after installing the P*trc*$_{core}$BCD-*ccr-phaJ* unit in strains BOH36 to BOH39, it was found that the P*trc*$_{2O}$ promoter for the *pduP-slr1192*^{OP} operon (strain BOH45) still worked best, and did not limit the 1-butanol production (ESI,† Fig. S8). The fact that a medium-strength expression level of PduP is beneficial for 1-butanol formation may be because the natural direction of PduP favors reversed butyryl-CoA formation.[24,25]

Based on the optimized constructs P*trc*$_{2O}$-*pduP-slr1192*^{OP} and P*trc*$_{core}$BCD-*ccr-phaJ* in strain BOH45, the performance of the *phaA*/*nphT7-phaB*^{T173S} operon under different promoters or 5′-regions was further investigated (Fig. 3c). Among the resultant strains BOH48 to BOH57, strain BOH56 harboring the P*trc*$_{core}$-RiboJ-*nphT7-phaB*^{T173S} unit had the largest improvement in the 1-butanol titer to 572 mg L^{-1}, a 5.3-fold increase compared with that of strain BOH45 (Fig. 3c), together with the highest protein expression levels of NphT7 and PhaB (ESI,† Fig. S7c). The 1-butanol titer of the NphT7 route in strain BOH56 was 0.5× higher than that of the PhaA route in strain BOH51 (374 mg L^{-1}), demonstrating that NphT7 in fact is not limited by the ACC reaction and malonyl-CoA level, and thus could more efficiently supply acetoacetyl-CoA.

By successively applying transcriptional and translational modification *via* promoters and 5′-regions in Module 2, 1-butanol production was greatly improved to 572 mg L^{-1} (strain BOH56), which was 2.3-fold higher compared to that of strain BOH28 in Module 1 (Fig. 3c). Combining Module 1 with Module 2, a further optimized 1-butanol biosynthetic pathway and 5′-regions of the three expression units were thus obtained, including an increase in the ratio of required NADPH/NADH to 3 : 1 (ESI,† Fig. S9). Our systematic evaluation at the transcriptional and translational levels clearly demonstrates the importance of the components and sequences of the 5′-regions in expression units.

Rewiring the carbon flux (Module 1 + 2 + 3)

In the previous modules described above, the *phaEC*, *acs*, and *pta* sites were selected as genomic integration loci for the three expression units (ESI,† Table S5). PHB accumulation, resulting from the irreversible conversion of intermediate (*R*)-3-hydroxybutyryl-CoA catalyzed by PHB synthase (PhaE and PhaC) in *Synechocystis*,[23] directly competes with 1-butanol biosynthesis (Fig. 1). Hence, *phaEC* is good choice of knock-out/integration site. In addition, as the building block of 1-butanol, acetyl-CoA can be interconverted to

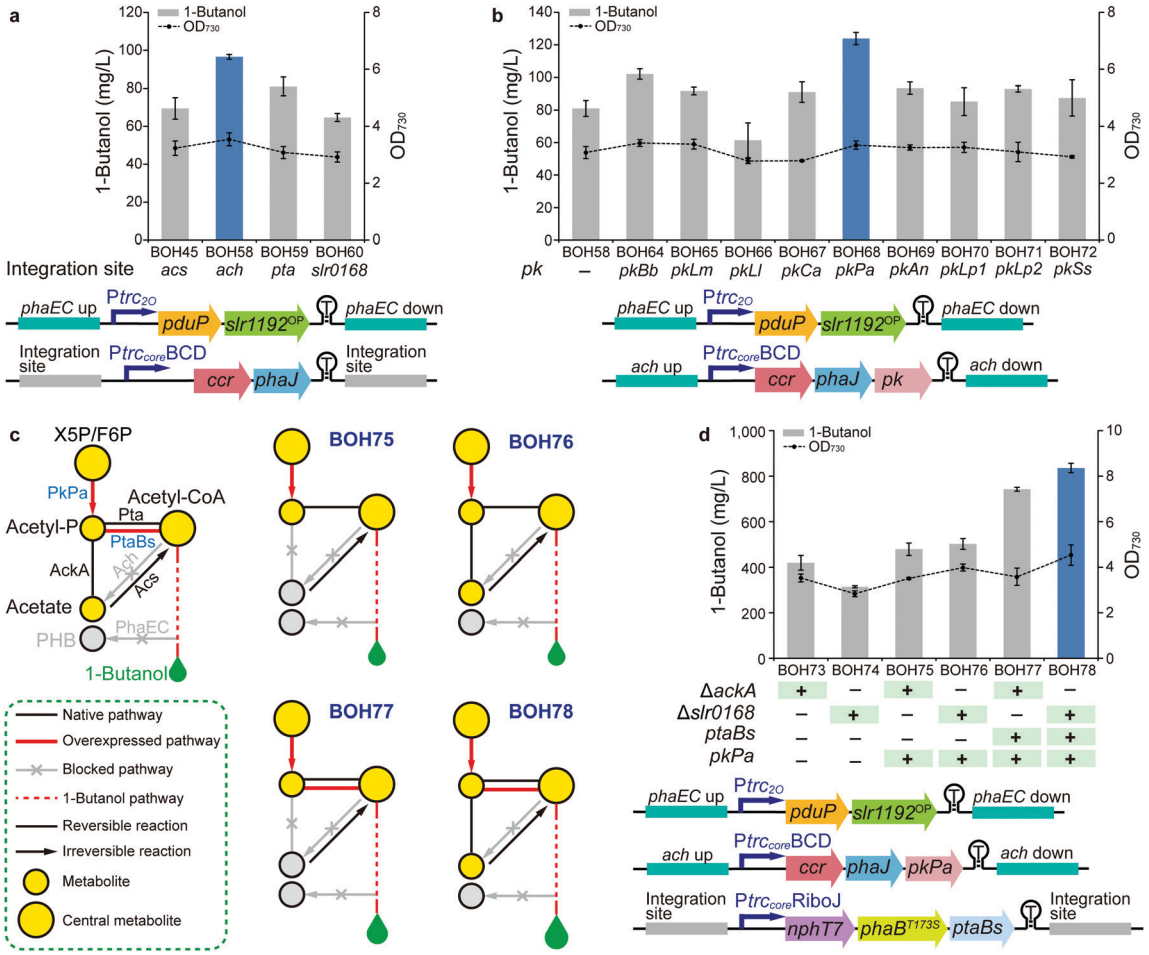

Fig. 4 Editing the acetate metabolism and installing the PK pathway in *Synechocystis* PCC 6803 (Module 1 + 2 + 3 + 4). (a) 1-Butanol production and cell density of strains BOH45 and BOH58–60 to compare four integration sites *via* the last four steps of the clostridial pathway. (b) 1-Butanol production and cell density of strains BOH58 and BOH64–72 to screen nine PKs *via* the last four steps of the clostridial pathway. (c) Simplified schematics of four rewiring and rewriting strategies in strains BOH75–78 by assembling Module 3 and 4. The pathway overview model in the left panel describes related metabolites, pathways and enzymes. Heterologous, endogenous and inactivated endogenous enzymes are shown in blue, black and grey fonts, respectively. See Fig. 1 regarding the abbreviations of the metabolites. (d) 1-Butanol production and cell density of strains BOH73–78 to compare six rewiring and rewriting strategies *via* the clostridial pathway. For (a, b and d), the time point, colored columns, " +", "–" and other detailed annotations are as described in the Fig. 2(b–e) legend. All data are presented as mean ± SD of biological triplicates. Genetic architectures of expression units are shown at the bottom of each panel.

acetate *via* the "triangular" acetate metabolism, consisting of the Pta (phosphotransacetylase), AckA (acetate kinase), Ach (acetyl-CoA hydrolase) and Acs (acetyl-coenzyme A synthetase) pathways (Fig. 1).[42] Since acetyl-CoA acts as the branching point for 1-butanol biosynthesis, acetate metabolism, and other competing metabolic pathways, the availability of acetyl-CoA may affect the carbon flux towards 1-butanol production.

Therefore, in Module 3, we manipulated the flow of acetyl-CoA by deleting genes responsible for the acetate metabolism to save this building block for 1-butanol biosynthesis. Furthermore, more possible genomic integration sites for integration of gene expression units were explored. 1-Butanol production levels were compared among strains using four integration loci, *acs* (strain BOH45), *ach* (strain BOH58), *pta* (strain BOH59), and the neutral site *slr0168*[43] (strain BOH60), for installing the P*trc*$_{core}$BCD-*ccr-phaJ* unit (Fig. 4a). Moreover, the expression unit of P*trc*$_{2O}$-*pduP-slr1192*^{OP} was placed at the *phaEC* site in all tested strains to allow functional 1-butanol production. Among the tested sites, the 1-butanol titer produced by strain BOH58 (96.5 mg L^{-1}) indicated that integration in and deletion of the *ach* site worked best (Fig. 4a). From western-immunoblotting data, the enzyme expression levels were comparable in all four strains (ESI,† Fig. S10), demonstrating that blocking the conversion of acetyl-CoA to acetate could enhance 1-butanol biosynthesis. The differences of 1-butanol production between strains with different knockouts in the acetate metabolism indicated that one of the key points in 1-butanol biosynthesis is most likely the cytosolic acetyl-CoA level.

Rewriting the central carbon metabolism (Module 1 + 2 + 3 + 4)

The main carbon flux in cyanobacterial cells, generated from the Calvin–Benson–Bassham (CBB) cycle, is channeled through the lower part of the glycolysis pathway, then *via* pyruvate to acetyl-CoA[9] (Fig. 1). The sugar catabolism (*e.g.* glycolysis

pathway) in *Synechocystis* is subject to regulation at the transcriptional level. Therefore, as the first experiment in Module 4, SigE, Rre37 and Hik8, known as positive transcriptional regulators of the sugar catabolism in *Synechocystis*,[44] were overexpressed to enhance 1-butanol production. However, when compared with strain BOH56, the introduction of the regulators in strains BOH61–63 did not exert a positive effect on 1-butanol production, and resulted in certain negative effects on protein expression levels (ESI,† Fig. S11).

Another strategy to increase the carbon flux *via* acetyl-CoA toward 1-butanol production is to install a phosphoketolase (PK) pathway (Fig. 1). PK catalyzes the cleavage of a 5-carbon xylulose-5-phosphate (X5P) into a 3-carbon glyceraldehyde-3-phosphate (G3P) and a 2-carbon acetyl-P, or a 6-carbon fructose-6-phosphate (F6P) into a 4-carbon erythrose-4-phosphate (E4P) and an acetyl-P.[45,46] This pathway enables a direct and irreversible conversion of sugar phosphate in the central carbon metabolism to acetyl-P and further on to acetyl-CoA, which is highly efficient when compared with the original acetyl-CoA synthesis *via* the glycolysis pathway. It also serves as a carbon-conserving shunt, compared to the carbon-wasting glycolysis pathway, in which one carbon is lost in the form of CO_2 with each acetyl-CoA generated from pyruvate[45] (Fig. 1). In cyanobacteria, where the carbon flux through the OPP (oxidative pentose phosphate) pathway is low under photoautotrophic conditions, the PK could divert X5P and F6P from the CBB cycle,[47] forming an effective shortcut from the CBB cycle to acetyl-P, and thus redirecting flux into 1-butanol biosynthesis (Fig. 1). Overexpression of a PK enzyme was shown to lead to higher production of PHB in one study in *Synechocystis*.[42] PK genes and the corresponding enzymes, which have previously been experimentally verified and characterized in several filamentous fungi, two cyanobacteria and some prokaryotic heterotrophic bacteria (ESI,† Table S3), display significant differences in their substrate specificities and catalytic kinetics towards X5P and F6P. Therefore, nine PKs were chosen as candidates to investigate their distinct efficiencies towards 1-butanol production (ESI,† Table S3). For the strain construction, each individual *pk* gene was cloned into the *ccr-phaJ* operon and integrated in the *ach* site, combined with the two optimized expression units selected in Module 3 (Fig. 4b). Among the nine resultant strains, BOH64-BOH72, the strain BOH68 overexpressing a PK from *Pseudomonas aeruginosa* (PKPa) had the highest 1-butanol titer, 124 mg L^{-1}, representing a 53% increase compared with that of strain BOH58 without PK overexpression (Fig. 4b). This is the first application of PKPa in metabolic engineering, and it represents a promising option of a PK for engineering biosynthetic pathways utilizing acetyl-CoA as a precursor.

After fixing the most efficient PKPa pathway, we then combined Module 3 and 4 to look for potential bottlenecks in the acetate metabolism for acetyl-CoA formation from acetyl-P that are increased by PK overexpression (Fig. 4c). For the formation of acetyl-CoA, there are two distinct routes, namely the Pta route and the AckA-Acs route. In the Pta-catalyzed route, acetyl-P is directly converted into acetyl-CoA, while the second route consists of two reactions catalyzed by AckA and Acs, in which acetyl-P is first converted into acetate and then forms acetyl-CoA (Fig. 1 and 4c). Improving the carbon flux from acetyl-P to acetyl-CoA *via* the Pta route seems to be a more effective strategy. Thus, the Pta from *Bacillus subtilis* (PtaBs), a shorter variant of Pta compared to the Pta found in *E. coli* and *Synechocystis*,[48] was selected to construct a synthetic PKPa-PtaBs route (Fig. 1 and 4c). Then, the PKPa or PKPa-PtaBs route was combined with the deletion of either *ackA* or the neutral site *slr0168*, resulting in strains BOH75–78 (Fig. 4c). Strains BOH73–74, lacking overexpressed PKPa, were constructed as controls. The difference between strain BOH75/77 and strain BOH76/78 was thus the blocked or open metabolic flux through the native AckA-Acs route. We conclude that combining PKPa and PtaBs enabled an enhanced carbon flux to acetyl-CoA, since strains BOH77/78 showed significantly higher 1-butanol production than strains BOH75/76 (Fig. 4d). Interestingly, the *slr0168*-deletion strain BOH78 generated a 13% increase in the 1-butanol titer (836 mg L^{-1}) compared with that of strain BOH77 harboring the *ackA* deletion (742 mg L^{-1}), probably because the native AckA-Acs route could provide additional flux from acetyl-P to acetyl-CoA. Hence, the optimal way to convert sugar to acetyl-CoA in *Synechocystis* is *via* a combination of the PKPa-PtaBs and PKPa-AckA-Acs routes (Fig. 4c).

From all information collected in the four modules of work described above, we conclude that the combined PKPa-PtaBs and PKPa-AckA-Acs routes are capable of efficiently diverting the carbon flux towards acetyl-CoA and drawing the equilibrium towards 1-butanol, when effectively irreversible steps have been implemented downstream in the 1-butanol biosynthetic pathway, such as the steps catalyzed by ACC, NphT7 and Ccr, and finally secretion of 1-butanol from the cells (ESI,† Fig. S12). The 1-butanol titer of strain BOH78, 836 mg L^{-1}, was at the conclusion of this part of our work the highest 1-butanol titer observed in cyanobacteria (ESI,† Table S1).

Long-term cultivation of BOH78

So far, we established, optimized and assembled four consecutive work modules with the best strain BOH78 producing 836 mg L^{-1} of 1-butanol (Fig. 5a and Fig. S12, ESI†). Then, the photosynthetic conditions in the sealed cultivation system were optimized to further enhance the 1-butanol titer of strain BOH78. A modified long-term cultivation of *Synechocystis* was set up using a pH adjustment approach[49] (ESI,† Fig. S13). The growth and 1-butanol production under different light intensities and $NaHCO_3$ feeding rates were examined for strain BOH78 and control strain EmptyV5 (ESI,† Fig. S14). The cell growth of strain BOH78 was slightly slower than the control, which maintained a longer steady state than strain BOH78, with no dramatic drop in growth in 30 days. Compared to the control, the effect of the light intensity on the cell growth of strain BOH78 was less significant, and strain BOH78 showed similar growth trends under two different $NaHCO_3$ feeding rates. The 1-butanol titer of strain BOH78 observed in cultures grown under 100 μmol photons m^{-2} s^{-1} was not enhanced compared to that in cultures grown under lower light intensities. We observed the highest 1-butanol titer from cells grown under 50 μmol photons m^{-2} s^{-1} with $NaHCO_3$ feeding every day. A maximal in-flask 1-butanol titer of

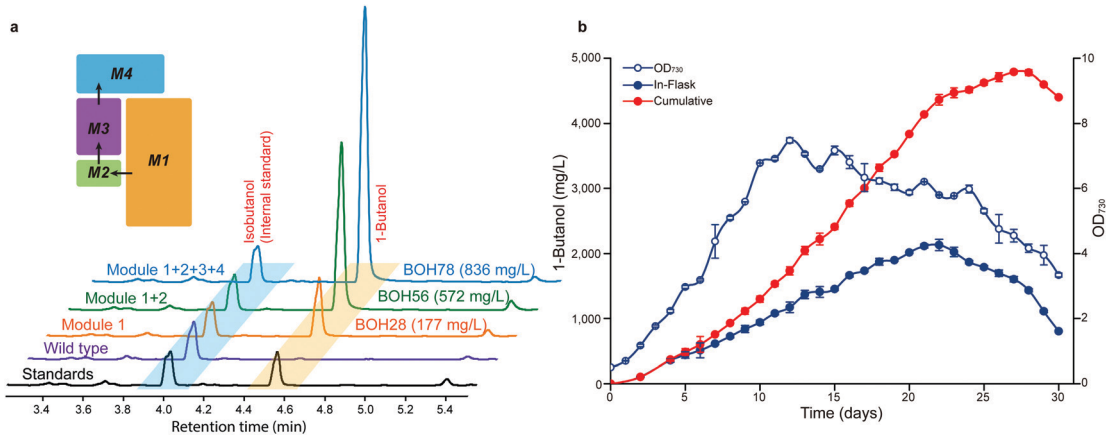

Fig. 5 Sequential improvements of 1-butanol production with four consecutive modules assembled and a long-term cultivation experiment for *Synechocystis* PCC 6803. (a) Representative gas chromatogram (GC) profiles of 1-butanol production from the best engineered strains in different combinatorial modules. The *Synechocystis* wild type is used as the negative control. The shown chromatogram is one of three similar traces from triplicate cultures. (b) Time course of OD_{730}, in-flask and cumulative 1-butanol production of strain BOH78 cultivated under a light intensity of 50 μmol photons m^{-2} s^{-1} with feeding $NaHCO_3$ every day for 30 days. The cumulative titer of 1-butanol takes into account the dilutions made to the cyanobacteria culture broth by feeding $NaHCO_3$. All data are presented as mean ± SD of biological triplicates.

2.13 g L^{-1} was observed at day 23 with a continuous decrease of the cell density from day 12 (Fig. 5b). This indicates that the cell growth does not correlate with the 1-butanol production levels. The 1-butanol concentration reached is higher than that observed to affect growth when 1-butanol was added externally to cells of *Synechocystis*.[50] However, the response may be different when the 1-butanol is produced internally. We continuously measured the 1-butanol production until day 30, when the cultivation was terminated due to a drop in the cumulative 1-butanol titer for the last two days. A final cumulative titer of 4.8 g L^{-1} 1-butanol at day 28 was obtained from strain BOH78. However, when feeding $NaHCO_3$ only every second day (ESI,† Fig. S14c), the maximal in-flask titer reached 1.86 g L^{-1} at day 23 with a cumulative titer of 3.0 g L^{-1} at day 26, demonstrating the importance of efficient removal of the produced 1-butanol.

The maximal 1-butanol production of 4.8 g L^{-1} is 11 times higher than previously reported in cyanobacteria, from engineered cells of *Synechococcus elongatus* PCC 7942, and even higher than the observed production when using engineered *Saccharomyces cerevisiae* (ESI,† Table S1). The average 1-butanol productivity during the 28 day cultivation period was 171 mg L^{-1} day^{-1}, with a maximal rate of 302 mg L^{-1} day^{-1} observed between days 15 and 18. The titer and rates of 1-butanol production reported in the present study are comparable with ethanol production (5.5 g L^{-1}, 212 mg L^{-1} day^{-1} during 26 days),[5] but higher than 2,3-butanediol production (2.38 g L^{-1}, 119 mg L^{-1} day^{-1} during 20 days)[13] and isoprene production (1.26 g L^{-1}, 60 mg L^{-1} day^{-1} during 21 days)[8] in cyanobacteria. However, ethanol, 2,3-butanediol and partly isoprene are pyruvate-derived products, whereas a higher alcohol like 1-butanol uses acetyl-CoA as the building block.

Conclusions

Throughout this work, our multi-level modular strategy transformed wild type *Synechocystis* cells into engineered *Synechocystis* strains with sequential improvements in 1-butanol production reaching 4.8 g L^{-1} with a maximal rate of 302 mg L^{-1} day^{-1} (Fig. 5a and 6). Various genetic modifications and multiple enzyme components, building on previous knowledge, were introduced in each work module and combined synergistically, allowing for fine design of the overall 1-butanol biosynthetic pathway. The designs used here are not limited to enhancing 1-butanol biosynthesis in cyanobacteria but can also be applied in metabolic engineering of other microorganisms, including *E. coli* and *S. cerevisiae*, for relevant chemicals production. Since some of the 1-butanol forming enzymes are widely applicable for the biosynthesis of other higher alcohols, acids or alkanes,[3,4,16,18,22,28,41] the genes and enzymes explored in our study can also be used in the biosynthesis of these acyl-CoA dependent products. The results from introducing and screening a large number of phosphoketolases (PK) will be useful for all applications requiring acetyl-CoA as a substrate.

Finally, we demonstrated the potential of cyanobacteria to be engineered as microbial cell factories, with a resulting product titer comparable with those achieved in heterotrophs. Our study contributes new insights to the field of metabolic engineering of cyanobacteria. Additional optimizations and use of dedicated automatic and continuous photobioreactor growth systems, operated in *e.g.* chemostat or turbidostat mode, in combination with product specific harvesting technologies including continuous removal of the products,[51] will make industrial biotechnological applications of cyanobacteria for direct production of chemicals and biofuels achievable.

Materials and methods

Plasmid construction

All the heterogenous genes and some endogenous genes were codon optimized and synthesized by GenScript. Other endogenous genes and DNA fragments (homologous recombination regions and $Pcpc_{560}$) were PCR amplified from the wild-type

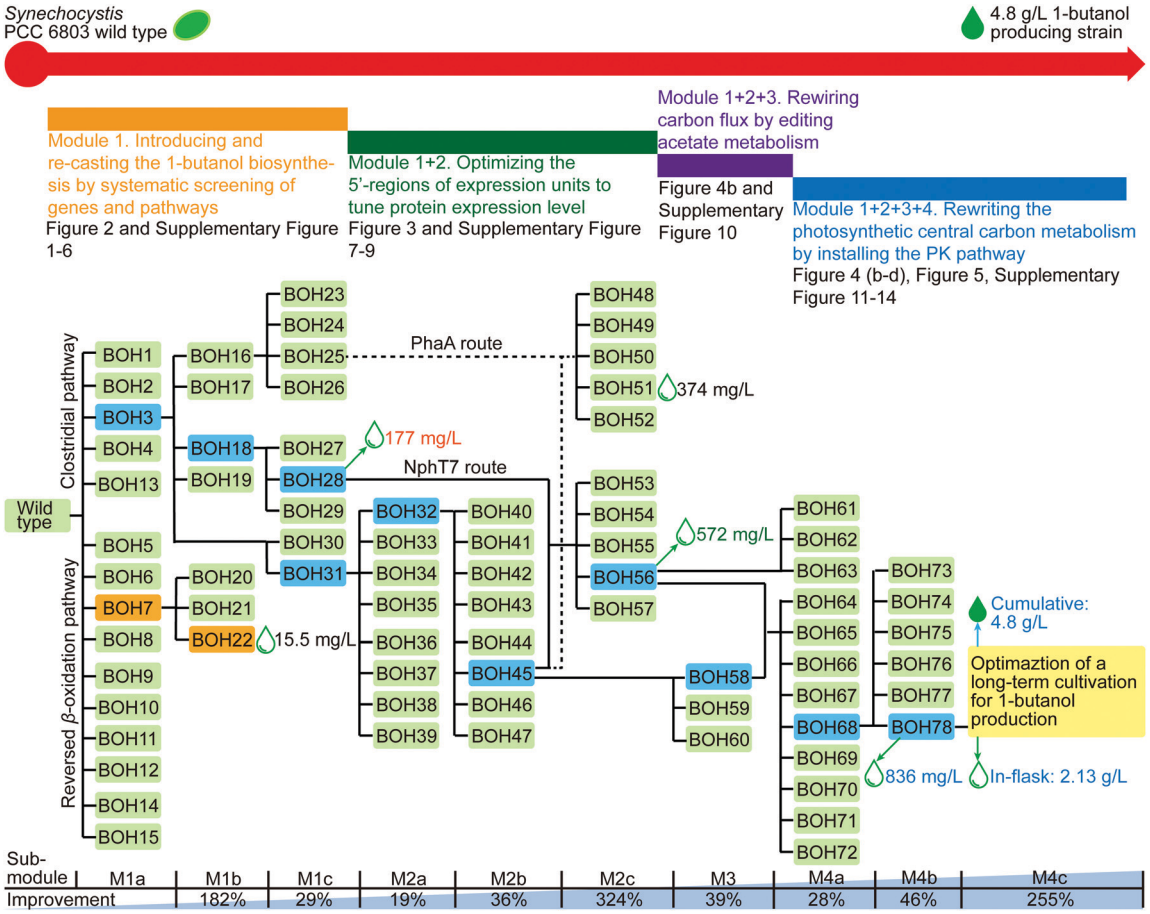

Fig. 6 Experimental development of 1-butanol producing *Synechocystis* strains through our multi-level modular engineering strategy. The blueprint of the process from the *Synechocystis* wild type to a 4.8 g L^{-1} 1-butanol producing strain is shown at the top, with the composition of combinatorial Modules 1, 2, 3 and 4. The related figures are listed below each Module part. The flowchart of strains with "laboratory evolution" is shown in the middle. This "genealogy map" include all the strains constructed in this study, by dividing them into different pathway and route schemes. The engineered strains connected to the next developed engineering stage or strains with the highest 1-butanol production in each step are highlighted in colors different from green. The target strains in the clostridial pathway and reversed β-oxidation pathway are shown in blue and orange, respectively. The detailed 1-butanol production of the best strains in the different pathways or combinatorial modules is also described beside. Sequential modifications in modules can be divided into different steps, called sub-modules. A diagram summarizing the sub-modules is shown in the lower part, together with a summary of stepwise improvements for in-flask 1-butanol production (in %) in *Synechocystis* PCC 6803.

Synechocystis PCC 6803 genome using gene specific primers and Phusion Polymerase (Thermo Fisher Scientific). The annotations of all genes, 5′-regions and other genetic elements are listed in the ESI,† Table S2. The sequences of codon optimized synthetic genes are listed in the ESI,† Table S7. P*psbA2*, RBS* and Terminator BBa_B0015 fragments were from pEERM1.[52] Ptrc_{2O}, Ptrc_{core}BCD and Ptrc_{core}RiboJ promotor fragments were amplified from pEEC series vectors.[53] The plasmids constructed in this study are listed in the ESI,† Table S4. The primers used in this study are listed in the ESI,† Table S6.

E. coli strain DH5α was used for constructing the plasmids containing P*psbA2* and Pcpc_{560}. *E. coli* strain DH5αZ1 (Invitrogen) was used for constructing the kanamycin or erythromycin resistance cassette carrying plasmids containing Ptrc_{2O}, Ptrc_{core}BCD or Ptrc_{core}RiboJ, while *E. coli* strain T7 Express (NEB) was used for constructing the spectinomycin resistance cassette carrying plasmids containing Ptrc_{2O}, Ptrc_{core}BCD or Ptrc_{core}RiboJ. All the strains were grown at 37 °C in LB medium (liquid or agar Petri dish) supplemented with the corresponding antibiotics (Sigma-Aldrich). Kanamycin, spectinomycin and erythromycin were used at a concentration of 50, 50, and 200 μg mL^{-1} for strains with the corresponding resistance marker, respectively. All the backbone vectors were made based on the recently reported pEERM series of vectors[52] by changing the homologous regions, promoters and antibiotic resistance cassettes with restriction enzyme digestion and ligation (ESI,† Table S4). The homologous recombination regions in all plasmids are the around 1000 bp upstream sequence and 1000 bp downstream sequence of the integrated gene locus. Further versions of the integrated plasmids were made based on existing backbone vectors with the BioBrick suffix and prefix for multi-step cloning[52] (ESI,† Table S4). Strong ribosome binding site RBS* was added in front of each gene, except the first gene behind the promoter, to allow initiation of translation. Bgl II, EcoR I, Xba I, Spe I, Pst I, BamHI and Sal I were the restriction cloning sites used to construct all the plasmids in this study. All digestion enzymes to cut the restriction cloning sites were fast digestion enzymes from

Thermo Fisher Scientific. *E. coli* colonies with positive plasmids were confirmed with colony PCR using gene specific primers (ESI,† Table S6) and DreamTaq DNA polymerase (Thermo Fisher Scientific). Plasmids purified with miniprep (Thermo Fisher Scientific) were checked by enzyme digestion before *Synechocystis* transformation.

Transformation of *Synechocystis*

The glucose-tolerant *Synechocystis* PCC 6803 (*Synechocystis*) strain was used in this study[27] (ESI,† Table S5). Transformation was performed by using a double homologous-recombination system, and the genes were integrated into the target site of the *Synechocystis* genomic DNA. The *Synechocystis* strains constructed in this study are listed in the ESI,† Table S5. Background strains (*Synechocystis* strains transformed with the corresponding backbone vectors) were used as a control for the engineered strains with genetic constructs on the chromosome. Kanamycin was used at a concentration of 50 μg mL^{-1} for strains with only the kanamycin resistance marker. For strains with multiple resistance markers, kanamycin, spectinomycin and erythromycin were used at 25 μg mL^{-1}.

Natural transformation with plasmids was performed *via* an optimized protocol based on previous reports.[54–60] *Synechocystis* cells were grown to the mid-log phase with OD_{730} = 0.5–1.2 in liquid BG11 medium. Then, the cell culture was collected by centrifugation at 5000 × *g* for 5 min and washed twice with fresh liquid BG11 medium without antibiotics, and finally resuspended into fresh liquid BG11 medium at a density of 1×10^9 cells·mL^{-1} (OD_{730} = 2.5). A total of 400 μL concentrated *Synechocystis* cells were mixed with 4 μg target plasmid DNA. After incubating under constant 50 μmol photons m^{-2} s^{-1} illumination at 30 °C for 4–5 hours, the cells were spread on membrane filters on BG11 agar plates without antibiotics for another 18–24 hours incubation under constant 50 μmol photons m^{-2} s^{-1} illumination at 30 °C. For colony selection and maintenance, the filters were changed onto new BG11 agar plates with the corresponding antibiotics and incubated under the same conditions. Isolated single colonies (transformants) were streaked on a new BG11 agar plate with the corresponding antibiotics, and were analyzed by PCR using gene specific primers (ESI,† Table S6) and DreamTaq DNA polymerase (Thermo Fisher Scientific) to verify successful integration of the expression cassette into the genomic DNA. Positive homologous recombinants were inoculated into 6-well plates and further cultivated in liquid BG11 medium with the corresponding antibiotics and propagated continuously until fully segregated. The segregation of each strain was examined by PCR using gene specific primers (ESI,† Table S6) and DreamTaq DNA polymerase (Thermo Fisher Scientific) on the extracted genome DNA prepared *via* an established protocol.[61]

Cultivation conditions for 1-butanol production

All experimental cultures were grown in BioLite 25 cm^2 plug-sealed tissue culture flasks (Thermo Fisher Scientific) to avoid 1-butanol evaporation during cultivation.[27] The $NaHCO_3$ supplemented was the inorganic carbon source for photosynthesis in *Synechocystis*. All experimental cultures were prepared in triplicate. Light was measured using an LI-190SB Quantum sensor.

Seed cultures of strains were grown under constant 50 μmol photons m^{-2} s^{-1} illumination at 30 °C in liquid BG11 medium with the corresponding antibiotics in 100 mL Erlenmeyer flasks (VWR) until the mid-log phase. For the HEPES-buffered cultures, each seed culture was then inoculated to OD_{730} = 0.1 with a total volume of 25 mL liquid medium in plug-sealed tissue culture flasks. The medium used was BG11 medium with 50 mM $NaHCO_3$ (Sigma-Aldrich), 25 mM HEPES (pH 7.5, Sigma-Aldrich) and the corresponding antibiotics. The initial OD_{730} was changed to 0.5 and the $NaHCO_3$ concentration was reduced to 20 mM for the cultivation of strains BOH48–57, BOH61–63 and BOH73–78 due to the specific phenotype of these strains. The flasks were shaken at 120 rpm, under constant 50 μmol photons m^{-2} s^{-1} illumination at 30 °C. 100 μL culture was sampled from each flask daily for OD_{730} measurements. An additional 2.3 mL culture was sampled from each flask every second day for 1-butanol extraction while 2.5 mL fresh BG11 medium with 500 mM $NaHCO_3$, 25 mM HEPES (pH 7.5) and the corresponding antibiotics was added back for filling up to the original volume. This procedure ensures a sustained carbon supply for *Synechocystis*. The cultivation was terminated when the 1-butanol titer in the culture began to decrease, and then the maximal in-flask 1-butanol titer was obtained.

In the long-term cultivation experiment, each seed culture was then inoculated to OD_{730} = 0.5 with a total volume of 25 mL liquid modified BG11 medium with 20 mM $NaHCO_3$ and the corresponding antibiotics. For examining different light intensities, the flasks were shaken at 120 rpm, at 30 °C, under constant 20, 50, and 100 μmol photons m^{-2} s^{-1}, respectively. 2.5 mL culture was sampled from each flask every day or every second day for OD_{730} measurements and 1-butanol extraction while 2.5 mL fresh BG11 medium with 500 mM $NaHCO_3$ and the corresponding antibiotics was added back for filling up to the original volume. For the HCl titrated cultures, a certain amount of 37% HCl (Sigma-Aldrich) was added every day to adjust the pH of the culture to around 7.5, which is close to the theoretical optimal pH for *Synechocystis*.[62] The pH was measured using MColorpHast™ pH-indicator strips (pH 6.5–10) (Merck). The detailed experimental procedure is shown in the ESI,† Fig. S13.

Optical density measurements and 1-butanol extraction

The cell growth was monitored by measuring the optical density at 730 nm (OD_{730}) of each culture. The absorbance at 730 nm was measured for 200 μL diluted culture every day in 96-well plates using a micro-plate reader (HIDEX, Plate Chameleon).

For 1-butanol extraction, 2.3 mL culture was centrifuged at 5000 rpm, for 10 min. Then, 2.07 mL supernatant was transferred into a 15 mL screw cap tube, and mixed with 30 μL 7000 mg L^{-1} internal standard isobutanol (Sigma-Aldrich) and 700 μL (1/3 volume) extraction solvent DCM (dichloromethane, Sigma-Aldrich). The mixture was shaken on a Multi-Tube Vortexer VX-2500 (VWR) at maximum speed for 5 min and then centrifuged at 5000 rpm, 4 °C, for 10 min, to get a faster and clearer separation of the two phases. The DCM phase (bottom phase) was transferred into 1.5 mL clear glass gas chromatography (GC) vials (VWR).

1-Butanol quantification by gas chromatography

The detection method was described in a previous study.[27] In short, the extracted samples were analyzed on a PerkinElmer GC 580 system equipped with a flame ionization detector (FID) and an Elite-WAX polyethylene glycol series capillary column, 30 m × 0.25 mm × 0.25 μm (PerkinElmer). Nitrogen was the carrier gas, with a 10 mL min^{-1} flow rate. The temperatures of the injector and detector were 220 °C and 240 °C, respectively. The initial oven temperature was 50 °C and then it was raised to 100 °C with a rate of 10 °C min^{-1} followed by a rise to 180 °C with a rate of 20 °C min^{-1}. The GC results were analyzed using TotalChrom Navigator version 6.3.2.

The retention time was determined using 100 mg L^{-1} isobutanol (Sigma-Aldrich) and 1-butanol standards (VWR). The chromatographic peaks of 1-butanol and isobutanol were indicated at a retention time of 4.55 min and 4 min, respectively, as shown in Fig. 5a. The presence of 1-butanol was identified by the retention time and comparison with the 1-butanol standard. All samples were spiked with the same amounts of isobutanol (100 mg L^{-1}), which was used as the internal standard for quantitative determination. Thus, a standard curve was made by measuring extracts (extracted in the same way as our samples) from liquid BG11 medium with nine different concentrations of the 1-butanol standard (10 mg L^{-1}, 25 mg L^{-1}, 50 mg L^{-1}, 75 mg L^{-1}, 100 mg L^{-1}, 250 mg L^{-1}, 500 mg L^{-1}, 750 mg L^{-1} and 1000 mg L^{-1}) and 100 mg L^{-1} of isobutanol as an internal standard. The amount of 1-butanol in the culture (in-flask titer of 1-butanol) was calculated based on the ratio of its signal peak area and that of the internal standard. The cumulative titer of 1-butanol takes into account the dilutions made to the cyanobacteria culture broth by feeding.

Crude protein extraction and Western-immunoblotting

The analyzed protein samples were the soluble fractions in the crude extract from the cell lysate of the engineered *Synechocystis* strains. Proteins extraction was done *via* a modified protocol based on a previous study.[63] 5 mL of culture was harvested from an OD_{750} = 2 culture by centrifugation at 4500 rpm, 4 °C, for 5 min. The pellet was washed in 2 mL PBS buffer and collected again by centrifugation at 4500 rpm, 4 °C, for 5 min. Then, 200 μL PBS buffer supplemented with 4 μL of 50× Protease Arrest (GBioscience) was used to resuspend the pellet and this mixture was frozen at −80 °C for 4 min followed by heating at 37 °C for 4 min. For the remainder of the procedure, the samples were kept on ice. Acid-washed glass beads (425–600 μm diameter, Sigma-Aldrich) were mixed with the thawed cells. The cells were disrupted using a Precellys-24 Beadbeater (Bertin Instruments); a 5000 rpm program for 4 × 30 s with 2 minutes of rest on ice between the runs is sufficient. 100 μL PBS buffer was added and the total lysates were briefly centrifuged twice at 1000 × *g*, 4 °C, 30 s, to get a supernatant containing soluble proteins.

The protein concentration was determined by the DC protein assay (Bio-Rad). 20 μg total soluble proteins from each strain were loaded in each lane and separated by running SDS-PAGE, using Mini-PROTEAN TGX™ gels (Bio-Rad), and transferred to a "Trans-Blot Turbo Transfer Pack" membrane (Bio-Rad) by a membrane transfer machine (Bio-Rad). Commercially available anti-Strep-tag antibody (abcam), anti-Flag-tag antibody (Sigma) and anti-His-tag antibody (Genscript) were used to detect the corresponding tagged protein through the standard techniques of immunoblotting. The annotations including the N-terminal tag of all enzymes are in the ESI,† Table S2.

Conflicts of interest

There are no conflicts to declare.

Acknowledgements

We thank Dr Xuefeng Lv (Qingdao Institute of Bioenergy and Bioprocess Technology, Chinese Academy of Sciences) for kindly providing the spectinomycin resistance cassette. This work was supported by the European Union Horizon 2020 Framework Programme under the grant agreement number 640720 (Photofuel), the Swedish Energy Agency (CyanoFuels, project number P46607-1), and the NordForsk NCoE program "NordAqua" (project number 82845).

References

1 A. Deneyer, E. Peeters, T. Renders, S. Van den Bosch, N. Van Oeckel, T. Ennaert, T. Szarvas, T. I. Korányi, M. Dusselier and B. F. Sels, *Nat. Energy*, 2018, **3**, 969–977.
2 Y. J. Zhou, E. J. Kerkhoven and J. Nielsen, *Nat. Energy*, 2018, **3**, 925–935.
3 S. Atsumi, W. Higashide and J. C. Liao, *Nat. Biotechnol.*, 2009, **27**, 1177–1180.
4 C. R. Shen and J. C. Liao, *Energy Environ. Sci.*, 2012, **5**, 9574–9583.
5 Z. Gao, H. Zhao, Z. Li, X. Tan and X. Lu, *Energy Environ. Sci.*, 2012, **5**, 9857–9865.
6 E. I. Lan, S. Y. Ro and J. C. Liao, *Energy Environ. Sci.*, 2013, **6**, 2672–2681.
7 W. Xiong, J. A. Morgan, J. Ungerer, B. Wang, P.-C. Maness and J. Yu, *Nat. Plants*, 2015, **1**, 15053.
8 X. Gao, F. Gao, D. Liu, H. Zhang, X. Nie and C. Yang, *Energy Environ. Sci.*, 2016, **9**, 1400–1411.
9 M. Kanno, A. L. Carroll and S. Atsumi, *Nat. Commun.*, 2017, **8**, 14724.
10 A. Wegelius, N. Khanna, C. Esmieu, G. D. Barone, F. Pinto, P. Tamagnini, G. Berggren and P. Lindblad, *Energy Environ. Sci.*, 2018, **11**, 3163–3167.
11 D. Lips, J. M. Schuurmans, F. Branco dos Santos and K. J. Hellingwerf, *Energy Environ. Sci.*, 2018, **11**, 10–22.
12 J. W. Lee, D. Na, J. M. Park, J. Lee, S. Choi and S. Y. Lee, *Nat. Chem. Biol.*, 2012, **8**, 536–546.
13 J. W. Oliver, I. M. Machado, H. Yoneda and S. Atsumi, *Proc. Natl. Acad. Sci. U. S. A.*, 2013, **110**, 1249–1254.
14 P. K. Ajikumar, W. H. Xiao, K. E. Tyo, Y. Wang, F. Simeon, E. Leonard, O. Mucha, T. H. Phon, B. Pfeifer and G. Stephanopoulos, *Science*, 2010, **330**, 70–74.

15 F. Zhang, J. M. Carothers and J. D. Keasling, *Nat. Biotechnol.*, 2012, **30**, 354–359.
16 H. C. Tseng and K. L. Prather, *Proc. Natl. Acad. Sci. U. S. A.*, 2012, **109**, 17925–17930.
17 P. Xu, Q. Gu, W. Wang, L. Wong, A. G. Bower, C. H. Collins and M. A. Koffas, *Nat. Commun.*, 2013, **4**, 1409.
18 M. J. Sheppard, A. M. Kunjapur, S. J. Wenck and K. L. Prather, *Nat. Commun.*, 2014, **5**, 5031.
19 J. Qin, Y. J. Zhou, A. Krivoruchko, M. Huang, L. Liu, S. Khoomrung, V. Siewers, B. Jiang and J. Nielsen, *Nat. Commun.*, 2015, **6**, 8224.
20 C. R. Shen, E. I. Lan, Y. Dekishima, A. Baez, K. M. Cho and J. C. Liao, *Appl. Environ. Microbiol.*, 2011, **77**, 2905–2915.
21 E. I. Lan and J. C. Liao, *Proc. Natl. Acad. Sci. U. S. A.*, 2012, **109**, 6018–6023.
22 C. Dellomonaco, J. M. Clomburg, E. N. Miller and R. Gonzalez, *Nature*, 2011, **476**, 355–359.
23 G. Taroncher-Oldenburg, K. Nishina and G. Stephanopoulos, *Appl. Environ. Microbiol.*, 2000, **66**, 4440–4448.
24 C. Fan, S. Cheng, Y. Liu, C. M. Escobar, C. S. Crowley, R. E. Jefferson, T. O. Yeates and T. A. Bobik, *Proc. Natl. Acad. Sci. U. S. A.*, 2010, **107**, 7509–7514.
25 C. Fan, S. Cheng, S. Sinha and T. A. Bobik, *Proc. Natl. Acad. Sci. U. S. A.*, 2012, **109**, 14995–15000.
26 J. W. Cooley and W. F. Vermaas, *J. Bacteriol.*, 2001, **183**, 4251–4258.
27 R. Miao, X. Liu, E. Englund, P. Lindberg and P. Lindblad, *Metab. Eng. Commun.*, 2017, **5**, 45–53.
28 Y. X. Huo, K. M. Cho, J. G. Rivera, E. Monte, C. R. Shen, Y. Yan and J. C. Liao, *Nat. Biotechnol.*, 2011, **29**, 346–351.
29 H. Liu, K. K. Wallace and K. A. Reynolds, *J. Am. Chem. Soc.*, 1997, **119**, 2973–2979.
30 S. Slater, T. A. Mitsky, K. L. Houmiel, M. Hao, S. E. Reiser, N. B. Taylor, M. Tran, H. E. Valentin, D. J. Rodriguez, D. A. Stone, S. R. Padgette, G. Kishore and K. J. Gruys, *Nat. Biotechnol.*, 1999, **17**, 1011–1016.
31 S. J. Sim, K. D. Snell, S. A. Hogan, J. Stubbe, C. Rha and A. J. Sinskey, *Nat. Biotechnol.*, 1997, **15**, 63–67.
32 A. Pohlmann, W. F. Fricke, F. Reinecke, B. Kusian, H. Liesegang, R. Cramm, T. Eitinger, C. Ewering, M. Potter, E. Schwartz, A. Strittmatter, I. Voss, G. Gottschalk, A. Steinbuchel, B. Friedrich and B. Bowien, *Nat. Biotechnol.*, 2006, **24**, 1257–1262.
33 E. Okamura, T. Tomita, R. Sawa, M. Nishiyama and T. Kuzuyama, *Proc. Natl. Acad. Sci. U. S. A.*, 2010, **107**, 11265–11270.
34 K. Matsumoto, Y. Tanaka, T. Watanabe, R. Motohashi, K. Ikeda, K. Tobitani, M. Yao, I. Tanaka and S. Taguchi, *Appl. Environ. Microbiol.*, 2013, **79**, 6134–6139.
35 E. J. Kim and K. J. Kim, *Biochem. Biophys. Res. Commun.*, 2014, **452**, 124–129.
36 P. Lindberg, S. Park and A. Melis, *Metab. Eng.*, 2010, **12**, 70–79.
37 H. H. Huang, D. Camsund, P. Lindblad and T. Heidorn, *Nucleic Acids Res.*, 2010, **38**, 2577–2593.
38 J. Zhou, H. Zhang, H. Meng, Y. Zhu, G. Bao, Y. Zhang, Y. Li and Y. Ma, *Sci. Rep.*, 2014, **4**, 4500.
39 V. K. Mutalik, J. C. Guimaraes, G. Cambray, C. Lam, M. J. Christoffersen, Q. A. Mai, A. B. Tran, M. Paull, J. D. Keasling, A. P. Arkin and D. Endy, *Nat. Methods*, 2013, **10**, 354–360.
40 C. Lou, B. Stanton, Y. J. Chen, B. Munsky and C. A. Voigt, *Nat. Biotechnol.*, 2012, **30**, 1137–1142.
41 Y. Dekishima, E. I. Lan, C. R. Shen, K. M. Cho and J. C. Liao, *J. Am. Chem. Soc.*, 2011, **133**, 11399–11401.
42 R. Carpine, W. Du, G. Olivieri, A. Pollio, K. J. Hellingwerf, A. Marzocchella and F. B. Santos, *Algal Res.*, 2017, **25**, 117–127.
43 A. Kunert, M. Hagemann and N. Erdmann, *J. Microbiol. Methods*, 2000, **41**, 185–194.
44 M. Azuma, T. Osanai, M. Y. Hirai and K. Tanaka, *Plant Cell Physiol.*, 2011, **52**, 404–412.
45 I. W. Bogorad, T. S. Lin and J. C. Liao, *Nature*, 2013, **502**, 693–697.
46 W. Xiong, T. C. Lee, S. Rommelfanger, E. Gjersing, M. Cano, P. C. Maness, M. Ghirardi and J. Yu, *Nat. Plants*, 2015, **2**, 15187.
47 J. Anfelt, D. Kaczmarzyk, K. Shabestary, B. Renberg, J. Rockberg, J. Nielsen, M. Uhlen and E. P. Hudson, *Microb. Cell Fact.*, 2015, **14**, 167.
48 E. Presecan-Siedel, A. Galinier, R. Longin, J. Deutscher, A. Danchin, P. Glaser and I. Martin-Verstraete, *J. Bacteriol.*, 1999, **181**, 6889–6897.
49 R. Miao, H. Xie and P. Lindblad, *Biotechnol. Biofuels*, 2018, **11**, 267.
50 J. Anfelt, B. Hallstrom, J. Nielsen, M. Uhlen and E. P. Hudson, *Appl. Environ. Microbiol.*, 2013, **79**, 7419–7427.
51 J. Wagner, D. Lee-Lane, M. Monaghan, M. Sharifzadeh and K. Hellgardt, *Algal Research*, 2018, **37**, 92–102.
52 E. Englund, J. Andersen-Ranberg, R. Miao, B. Hamberger and P. Lindberg, *ACS Synth. Biol.*, 2015, **4**, 1270–1278.
53 E. Englund, K. Shabestary, E. P. Hudson and P. Lindberg, *Metab. Eng.*, 2018, **49**, 164–177.
54 S. S. Golden, J. Brusslan and R. Haselkorn, *Methods Enzymol.*, 1987, **153**, 215–231.
55 R. D. Porter, *Methods Enzymol.*, 1988, **167**, 703–712.
56 J. G. K. Williams, *Methods Enzymol.*, 1988, **167**, 766–778.
57 W. Vermaas, *J. Appl. Phycol.*, 1996, **8**, 263–273.
58 C. Jansson, G. Salih, J. Eriksson, R. Wiklund and H. Ghebramedhin, *Methods Enzymol.*, 1998, **297**, 166–182.
59 X. Zang, B. Liu, S. Liu, K. K. Arunakumara and X. Zhang, *J. Microbiol.*, 2007, **45**, 241–245.
60 B. Wang, J. Yu, W. Zhang and D. R. Meldrum, *Appl. Environ. Microbiol.*, 2015, **81**, 8500–8506.
61 P. Tamagnini, O. Troshina, F. Oxelfelt, R. Salema and P. Lindblad, *Appl. Environ. Microbiol.*, 1997, **63**, 1801–1807.
62 J. J. Huang, N. H. Kolodny, J. T. Redfearn and M. M. Allen, *Arch. Microbiol.*, 2002, **177**, 486–493.
63 N. B. Ivleva and S. S. Golden, *Methods Mol. Biol.*, 2007, **362**, 365–373.